Supporting Information

Oxygen-modified Ru for efficient alkaline hydrogen evolution reaction

Youpeng Cao,[a] Xingshuai Lv,[a] Jiao Yang,[a] Keyu An,[a] Chunfa Liu,[a] Lulu Qiao,[a] Zhichao Yu,[a] Lun Li,[a] and Hui Pan *[ab]

[a] Institute of Applied Physics and Materials Engineering, University of Macau, Macao SAR, 999078, China

[b] Department of Physics and Chemistry, Faculty of Science and Technology, University of Macau, Macao SAR, 999078, China

* Corresponding author.

Hui Pan: huipan@um.edu.mo (e-mail), +853 88224427 (tel.)

Experimental section

1 Chemicals.

Triruthenium dodecacarbonyl ($Ru_3(CO)_{12}$, >98%) was purchased from Bidepharm. Nafion perfluorinated resin solution (5 wt%) were purchased from Sigma Aldrich. Oleylamine ($C_{18}H_{37}N$, 80%-90%) was purchased from Macklin. Commercial Pt/C (20 wt% Pt) were purchased from TANAKA. Ethanol (C_2H_6O, AR), hexamethylene (C_6H_{12}, AR), isopropanol (C_3H_8O, AR) and potassium hydroxide (KOH, AR) were purchased from Aladdin. Vulcan carbon XC-72R was purchased from CABOT. All the chemicals were used without further purification. The deionized water (18 MΩ cm^{-1}) used in all the experiments was obtained by passing through an ultra-pure purification system (Aqua Solutions).

2 Synthesis of Ru nanocrystals and Ru/C

In a typical synthesis of Ru nanocrystals, 21 mg $Ru_3(CO)_{12}$ and 5 mL oleylamine were added into a glass vial (30 mL) and ultrasonicated for 0.5 h to form a homogeneous solution. The mixture was then heated to 200 °C and held at the same temperature for 6 h in oven. After cooling down to room temperature, 0.9 mL of reaction mixture was taken and washed with a mixture of ethanol/cyclohexane (8/1) for 3 times. The as-obtained nanocrystals were added into the cyclohexane (9 mL) with 12 mg XC-72R and ultrasonicated for 1 h.

2.1 Synthesis of Ru/C-200

Ru/C-200 was prepared by annealing Ru/C at 200 °C in air for 1 h.

2.2 Synthesis of Ru/C-220

Ru/C-220 was prepared by annealing Ru/C at 220 ℃ in air for 1 h.

2.3 Synthesis of Ru/C-240

Ru/C-240 was prepared by annealing Ru/C at 240 ℃ in air for 1 h.

2.4 Synthesis of NiFe LDH @ Ni felt. The Ni felt substrate (dimensions: 10 × 10 × 0.3 mm) underwent surface purification through sequential exposure to 2 M acetic acid (to eliminate oxide layers) followed by 10-minute ultrasonication in ethanol and deionized water. NiFe layered double hydroxide (LDH) was prepared by modifying an established procedure.[1, 2] A mixture was formulated by dissolving 0.5 mmol $Ni(NO_3)_2·6H_2O$, 0.5 mmol $Fe(NO_3)_3·9H_2O$, and 5 mmol $CO(NH_2)_2$ in 36 mL of deionized water, stirred until fully uniform. The pre-treated Ni felt was submerged in this solution inside a 50 mL Teflon-lined stainless-steel autoclave, subjected to heating at 120 °C for 12 hours, and subsequently allowed to cool naturally to ambient temperature. The Ni felt, now coated with LDH, was washed with deionized water and ethanol, then dried in a vacuum oven at 60 °C for 6 hours.

3 Materials characterizations

Phase identification was performed by X-ray diffraction (XRD) analysis. The XRD patterns were obtained from a Rigaku SmartLab SE diffractometer by scanning the angular range $5° \leq 2\theta \leq 90°$ using Cu Kα radiation ($\lambda = 1.5418$ Å). X-ray photoelectron spectroscopy (XPS) was obtained using a Thermo Scientific Escalab 250Xi spectrometer. The morphology and microstructure of the as-obtained samples were evaluated using transmission electron microscopy (TEM, JEM2010-HR). Raman spectra were recorded with a LABHRev-UV Raman spectrometer ranging from 200 to 1800 cm^{-1}. Electron paramagnetic resonance (EPR) spectra were collected on a Magnettech MS 5000 EPR spectrometer operating at room temperature with a micro frequency of 9.86 GHz. The inductively coupled plasma-mass spectrometry (ICP-MS) tests were performed on Agilent 7850, determining the weight ratios of Ru/C and Ru/C-220 determined to be 28.4% and 29.2%, respectively.

4 Electrochemical measurements

All the electrochemical measurements were tested on the electrochemical station (CHI760, Shanghai Chenhua) with a three-electrode system. The working electrode is a glassy carbon disk electrode, and graphite rod and mercuric oxide electrode were used the counter electrode and the reference electrode, respectively. For the preparation of the working electrode, Ru/C-220 (2 mg), Ru/C (2 mg) and Pt/C (2 mg), water (245 μL), isopropanol (745 μL), and Nafion solution (10 μL, 5 wt%) were mixed and ultrasonicated for 1 h to form a homogeneous ink. Afterwards, 12 μL ink was dropped on the glassy carbon disk electrode with a Ru loading of 0.035 mg cm^{-2}, a Pt loading of 0.024 mg cm^{-2}. The equilibrium potential was determined by the zero point of HER/HOR using Platinum working electrode as working electrode at 1600 r min^{-1} in H_2-saturated electrolyte. The linear sweep voltammetry (LSV) was performed at a scan rate of 5 mV s^{-1} with 95% ohmic drop compensation. Before each electrochemical test, the electrodes were swept with 25 cyclic voltammetry at 0.5 V s^{-}

^{1} to stabilize the catalysts' double layers and ensure complete wetting. Electrochemical impedance spectroscopy (EIS) measurements were conducted at a HER overpotential of 50 mV in the range from 100 kHz to 0.01 Hz. The stability of catalyst for HER was measured by drop-casting the catalyst on a carbon paper with a mass loading (Ru/C-220) of 0.24 mg cm^{-2}. The electrical double layer capacitance (C_{dl}) of the catalysts was estimated by testing CVs (Fig. S11) at different scan rates (ν) in the potential range of 0.925-1.125 V (vs. RHE). The C_{dl} values were calculated by the slope of $\Delta i/2$ vs ν plot ($\Delta i = i_{anode} - i_{cathode}$; extracted at 1.025 V vs. RHE), where i stands for the current from LSV.

For CO-stripping, CO was bubbled into aqueous KOH solution (1 mol L^{-1}) for 15 min. After the electrolyte was saturated with N_2 for 15 min, two cyclic voltammetry (CV) curves were collected at a scan rate of 20 mV s^{-1}.

The ECSA calculated by CO-stripping can be calibrated as:

$$ECSA = \frac{S_{Area}}{V_{Scan} \times 0.42 \times [M_{metal}]}$$

where M_{metal} is the mass loading of metal on a certain geometric area of the working electrode.

For the Cu stripping experiments, a N_2-saturated solution containing 50 mM $CuSO_4$ and 0.5 M H_2SO_4 was used as the electrolyte. The potential was first held at 0.3 V versus RHE for 100 s to form a Cu deposition monolayer, and then CVs were obtained from 0.3 V to 1.0 V at 20 mV s^{-1}. The ECSAs were calculated by subtracting the background CVs that were collected in N_2-saturated 0.5 M H_2SO_4 at 20 mV s^{-1}, assuming a charge density of 420 μC cm^{-2}.

The ECSA can be calibrated as:

$$ECSA = \frac{Q_{Cu}}{0.42 \times [M_{metal}]} = \frac{S_{Area}}{V_{Scan} \times 0.42 \times [M_{metal}]}$$

where M_{metal} is the mass loading of metal on a certain geometric area of the working electrode.

5 Electrochemical measurements in AEMWE device.

The anion exchange membrane water electrolyzer (AEMWE) comprising a cathode (Ru/C-220 and Pt/C deposited on carbon paper), an anode (NiFe LDH coated on Ni felt), and a commercial anion exchange membrane (X37-50, Sustainion from Dioxide Materials). The membrane underwent pretreatment by immersion in a 1 M KOH solution for a minimum of 10 hours. Catalyst ink for the cathode was applied to the carbon paper via air-spraying, targeting a loading of approximately 0.2 mg cm^{-2} for both Ru and Pt. The membrane electrode assembly (MEA) was assembled by sandwiching the cathode, pretreated membrane, and anode between two titanium bipolar plates, secured with a torque of 10 N m. The electrolyzer featured an active area of 1 cm^{2}. A 1 M KOH electrolyte was circulated through the system at a flow rate of 15 mL min^{-1} using a peristaltic pump (DIPump550-B253, Kamoer). The electrolyzer was preconditioned by operating at 50 mA cm^{-2} for 1 hour prior to measurements. To evaluate AEMWE performance, polarization curves were obtained by incrementally adjusting the current density from 0.02 A cm^{-2} to 1.0 A cm^{-2} at 60 °C, using a battery testing apparatus (ME-1S200, Kolibrik). Long-term stability was assessed by maintaining a steady current density of 0.45 A cm^{-2} at 25 °C. All electrochemical data from the AEMWE were collected without applying iR compensation.

6 Calculational details

First-principles calculations were performed based on the density-functional-theory (DFT) as implemented in the Vienna *ab initio* simulation package (VASP)[3, 4]. Core–valence interactions were described using the projector augmented wave (PAW)[5] method. The Perdew-Burke-Ernzerhof (PBE) functional[6] within the generalized gradient approximation (GGA) was used to treat the exchange−correlation interactions. All structures were relaxed utilizing a cutoff energy of 450 eV, and the convergence threshold was set to 10^{-5} eV and 0.02 eV/Å for energy and force[4], respectively. Grimme's DFT-D3 scheme of dispersion correction was adopted to consider the van der Waals (vdW) interaction in all systems. A smear of 0.1 eV at the Fermi level was used for geometric structure relaxation, while the density of states (DOS) was investigated with a reduced smear width of 0.05 eV. The kinetic barrier of water dissociation was calculated using the Climbing Image Nudged Elastic Band (CI-NEB) method[7]. Total energy and force threshold for geometry optimizations were 10^{-5} eV and 0.1 eV/Å, respectively. Four images were selected for transition state (TS) search, and each transition state is confirmed with a single imaginary vibrational frequency. The 2 × 1 supercell of Ru (101) surface was chosen as the structural model to represent the pristine Ru surface, where the bottom two layers of the slab were fixed at bulk lattice constant and the top two layers were allowed to relax. The oxidized Ru catalyst was built by partially oxidizing the surface Ru with oxygen atoms. A Monkhorst-Pack *k*-point mesh of 9 × 9 × 1 was sampled for the total energy calculation to give well converged energy values[8]. The periodic images in the *z*-direction were separated by 15 Å of vacuum space.

The Gibbs free energies were calculated according to:

$$G = E + \mathrm{ZPE} - TS$$

where E is the electronic energy calculated by DFT, ZPE denotes the zero-point energy estimated within the harmonic approximation, and TS is the entropy at 298.15 K (T = 298.15 K).[9] The zero-point energies and entropies of the reaction species were calculated from the vibrational frequencies. All atoms of substrate were rigid during these frequency computations. Based on the computational hydrogen electrode (CHE) model, the chemical potential of a proton and electron pair equivalent to that of a half of gaseous H_2 under standard condition.

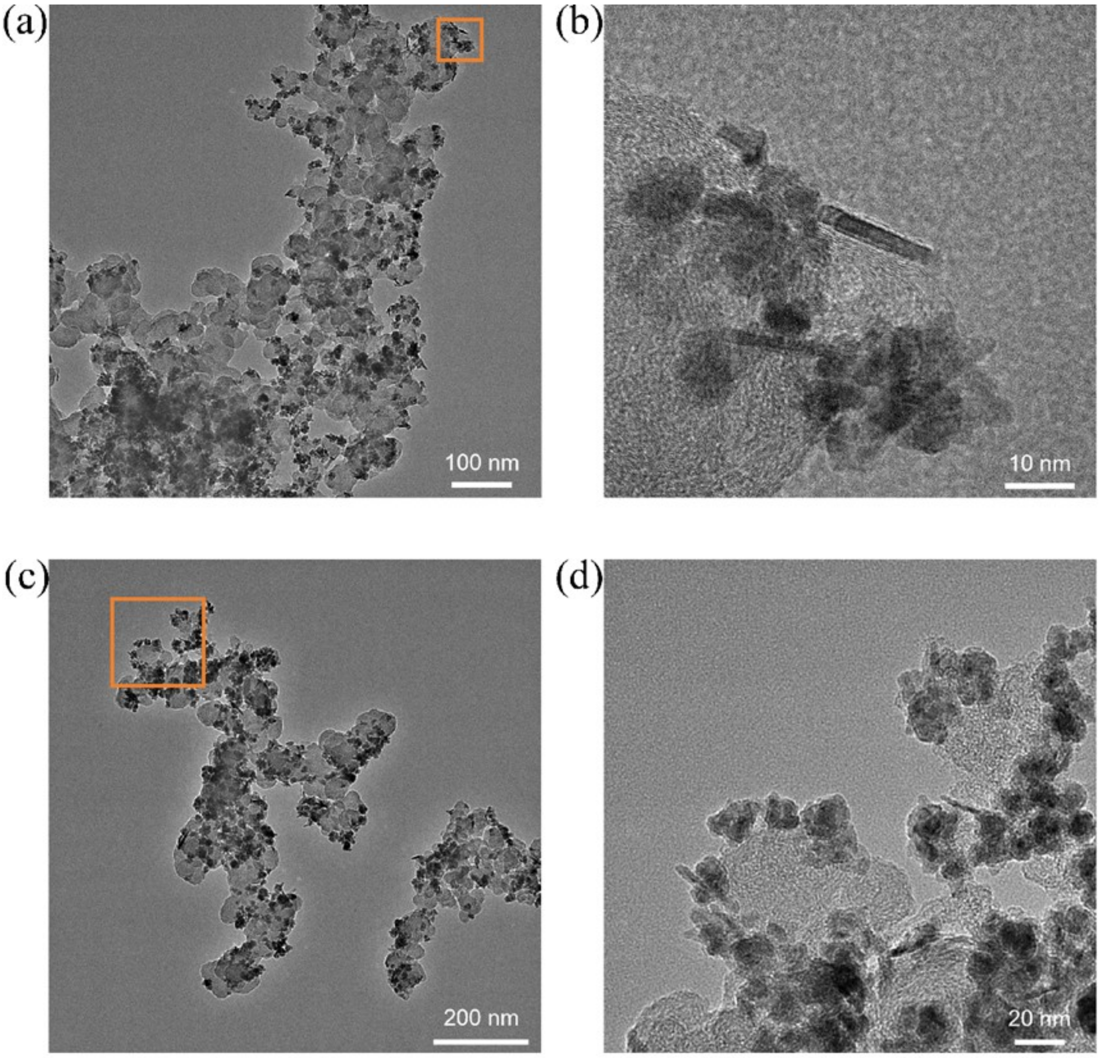

Fig. S1. TEM images of (a) Ru/C and (c) Ru/C-220. (b) Enlarged TEM image of the area indicated in (a). (d) Enlarged TEM image of the area indicated in (c).

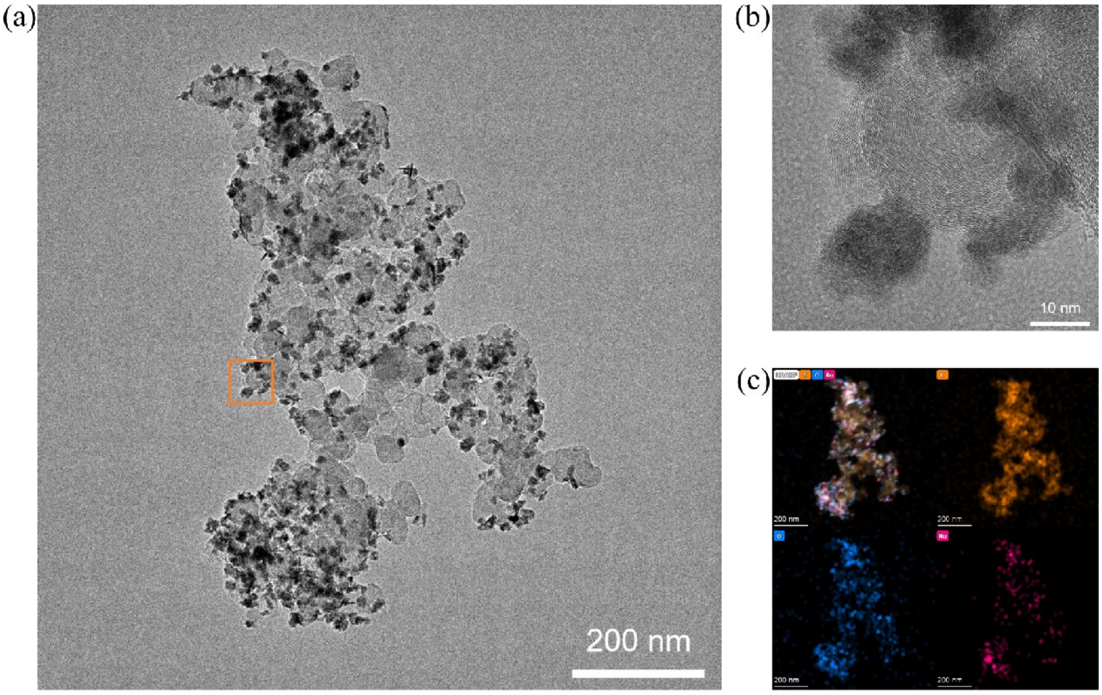

Fig. S2. TEM images of (a) Ru/C-200. (b) Enlarged TEM image of the area indicated in (a). (c) The corresponding EDS mapping of Ru/C-200.

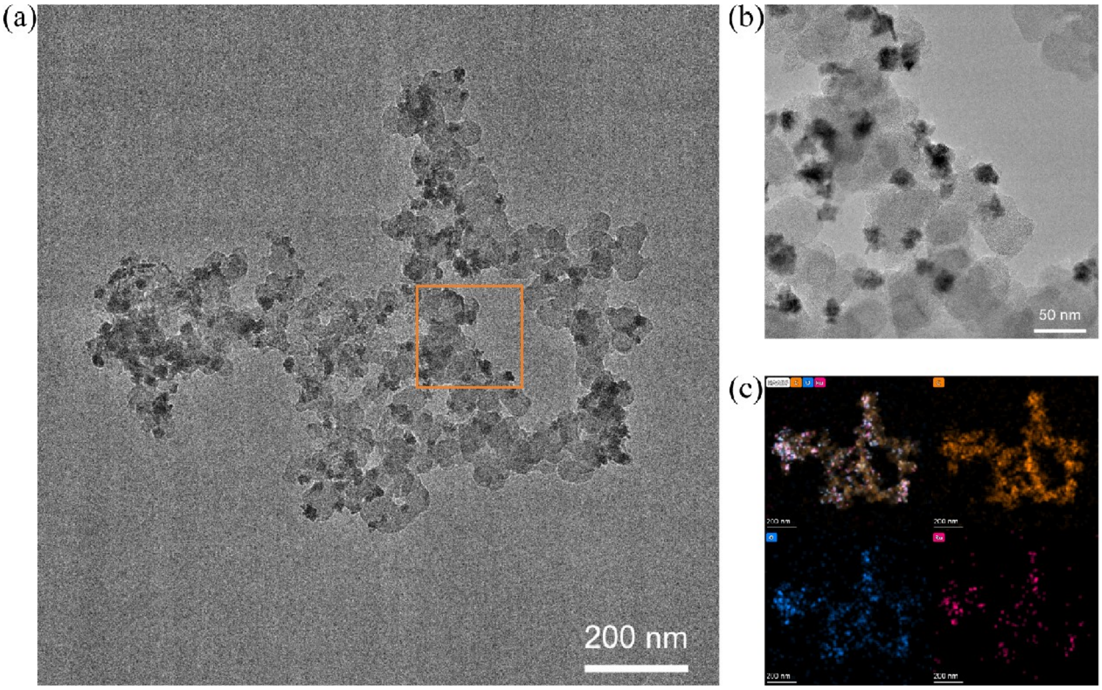

Fig. S3. TEM images of (a) Ru/C-240. (b) Enlarged TEM image of the area indicated in (a). (c) The corresponding EDS mapping of Ru/C-240.

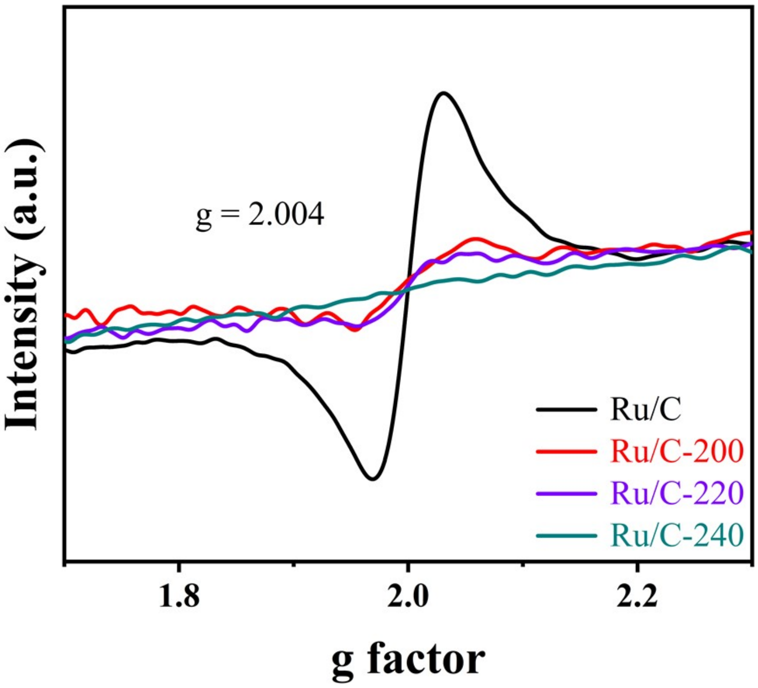

Fig. S4. EPR spectra of Ru/C, Ru/C-200, Ru/C-220 and Ru/C-240.

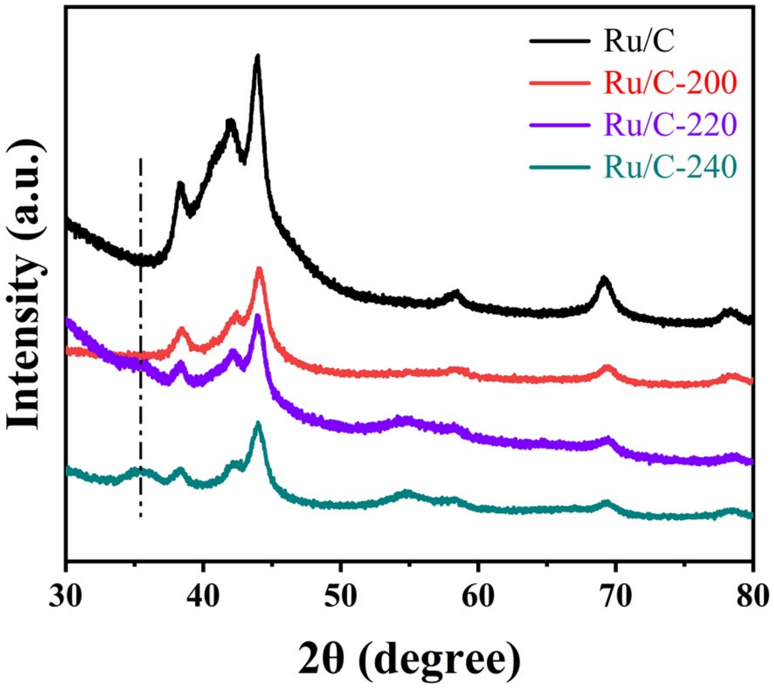

Fig. S5. XRD patterns of Ru/C, Ru/C-200, Ru/C-220 and Ru/C-240.

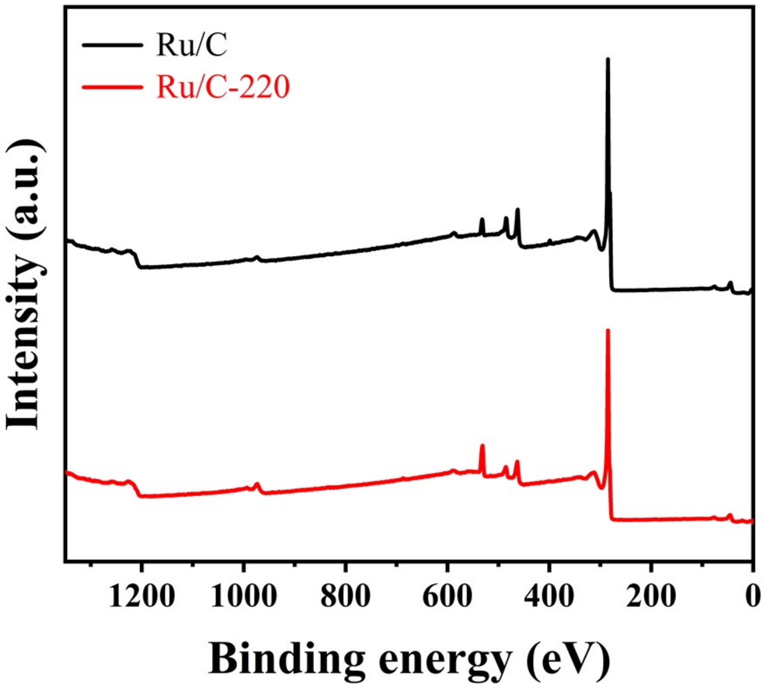

Fig. S6. XPS full spectra of Ru/C and Ru/C-220.

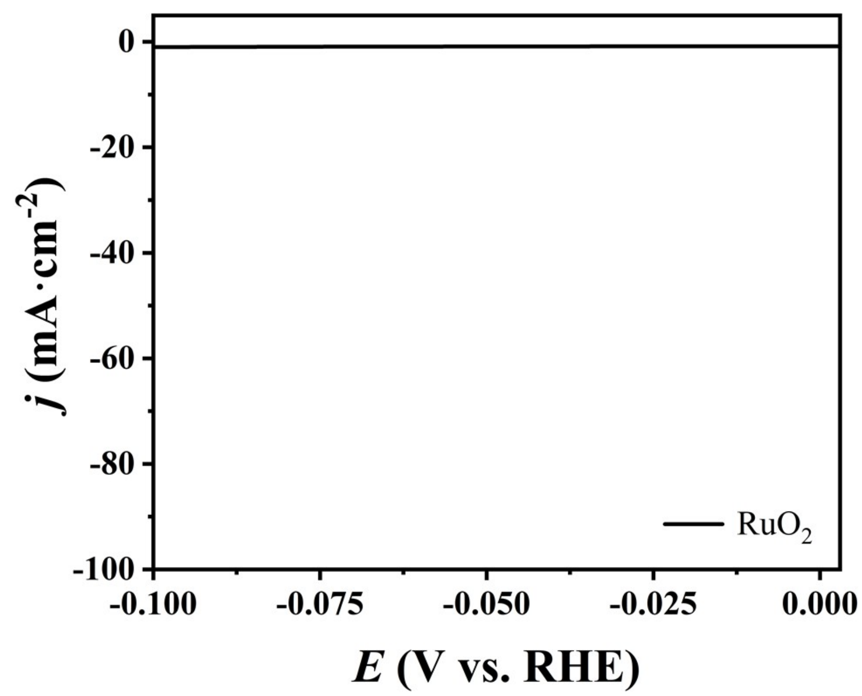

Fig. S7. HER polarization curves of commercial RuO_2 with 95% *iR* correction in a N_2-saturated 1 M KOH electrolyte with a rotating speed of 1,600 rpm.

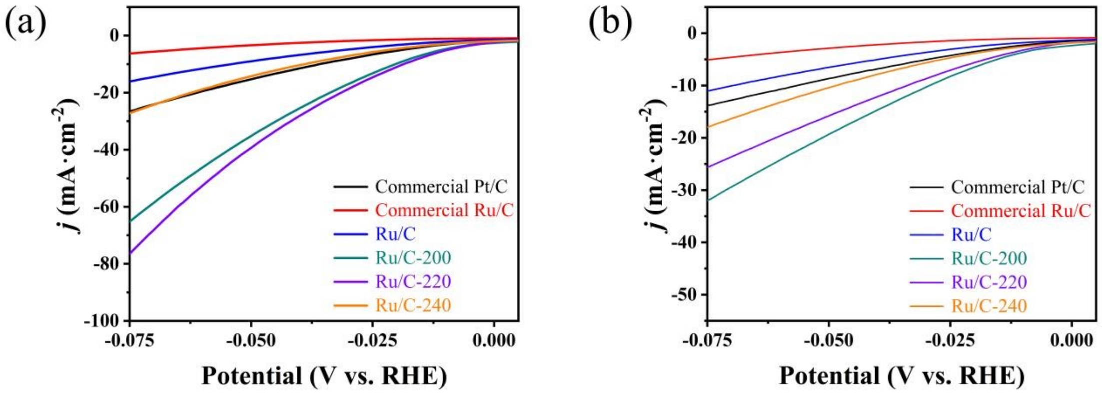

Fig. S8. HER polarization curves of Commercial Pt/C, Commercial Ru/C, Ru/C, Ru/C-200, Ru/C-220, and Ru/C-240 (a) with 95% *iR* correction (b) without *iR* correction in a N_2-saturated 1 M KOH electrolyte with a rotating speed of 1,600 rpm.

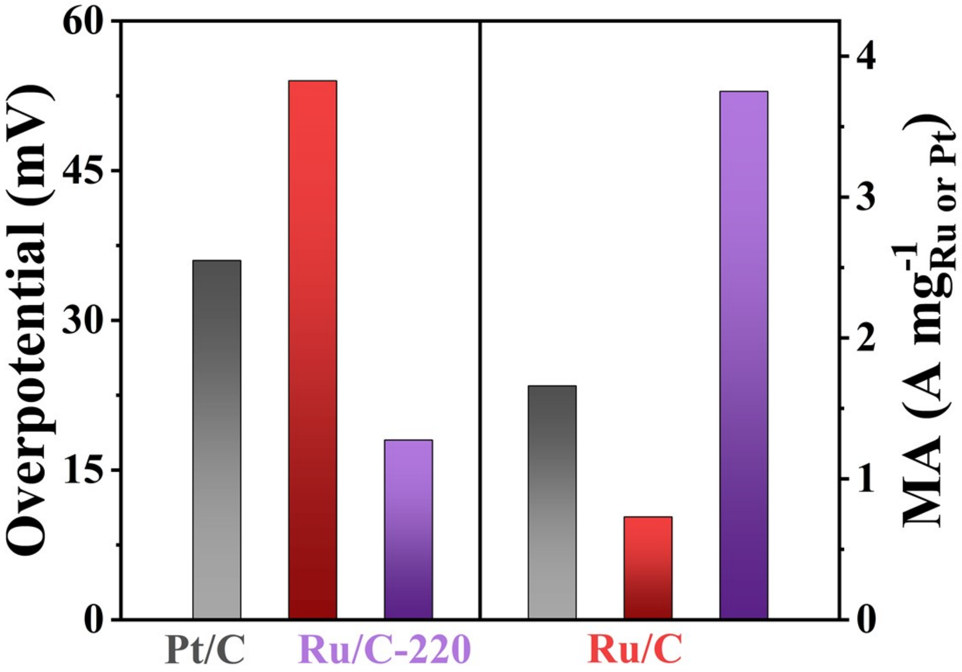

Fig. S9. Comparison of overpotential at 10 mA cm^{-2} and mass activity (MA) at 100 mV of different catalysts for HER.

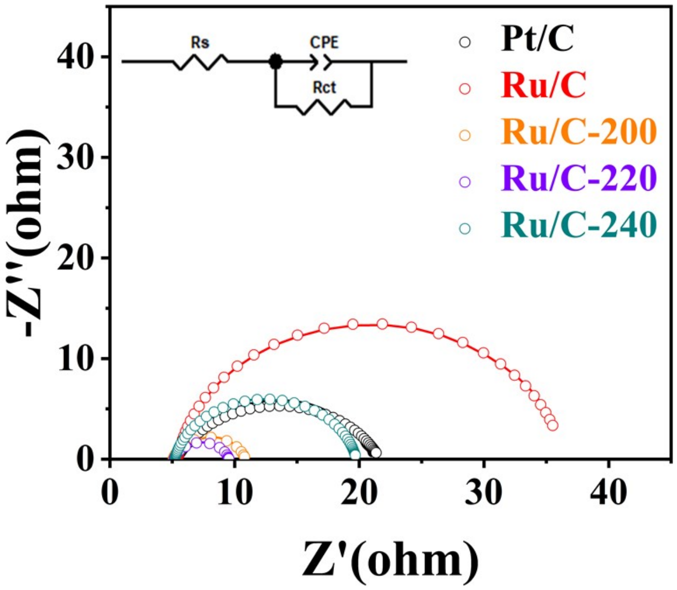

Fig. S10. Electrochemical impedance spectra of Pt/C, Ru/C, Ru/C-200, Ru/C-220 and Ru/C-240 from 100 kHz to 0.01 Hz (R_s: solution resistance, R_{ct}: charge transfer resistance, CPE: constant phase element. Dotted lines show fitted curves; solid lines represent experimental data.).

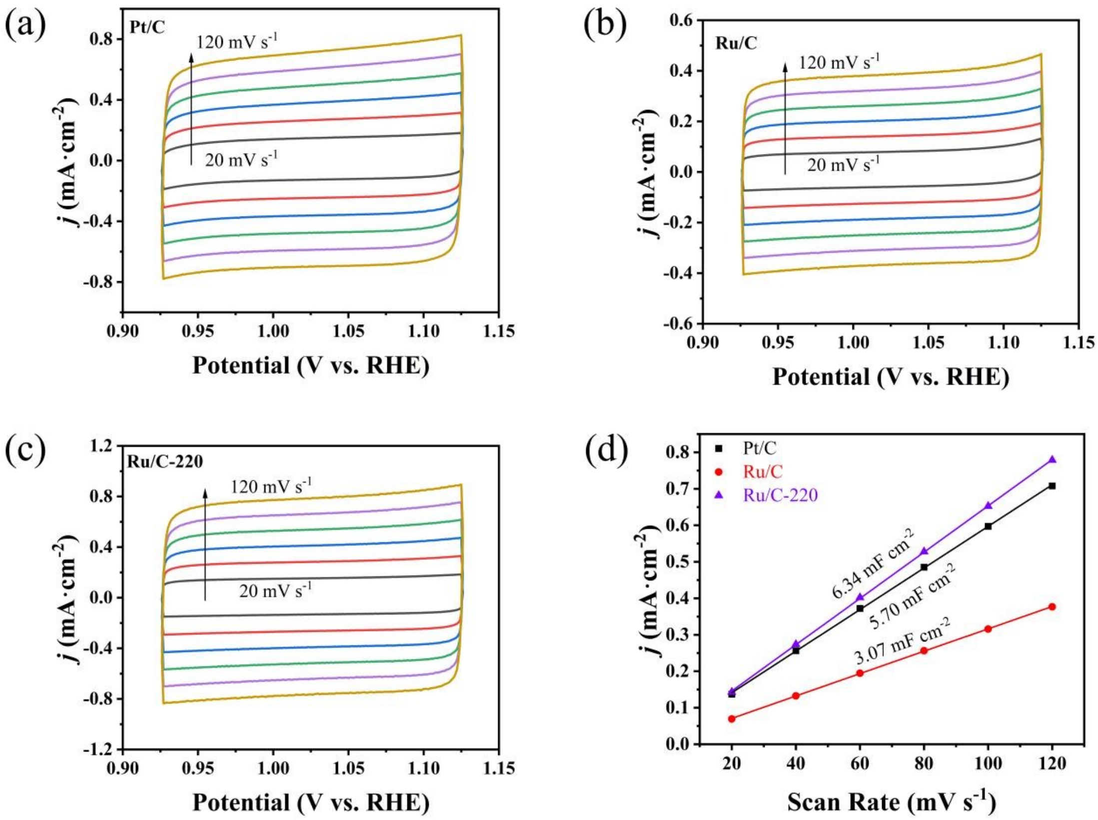

Fig. S11. Cyclic Voltammetry of different electrocatalysts in N_2-Saturated 1.0 M KOH. CV plots at varying scan rates from 20 to 120 mV s^{-1} of (a) Pt/C, (b) Ru/C, (c) Ru/C-220, (d) Double-layer capacitance (C_{dl}) of Pt/C, Ru/C and Ru/C-220

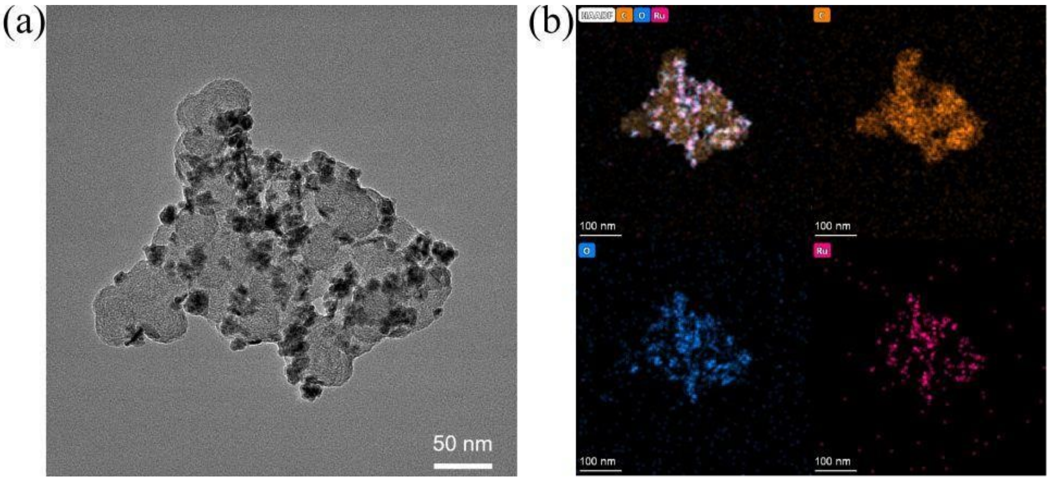

Fig. S12. TEM images of (a) Ru/C-220 after stability tests. (b) The corresponding EDS mapping of Ru/C-220 after stability tests.

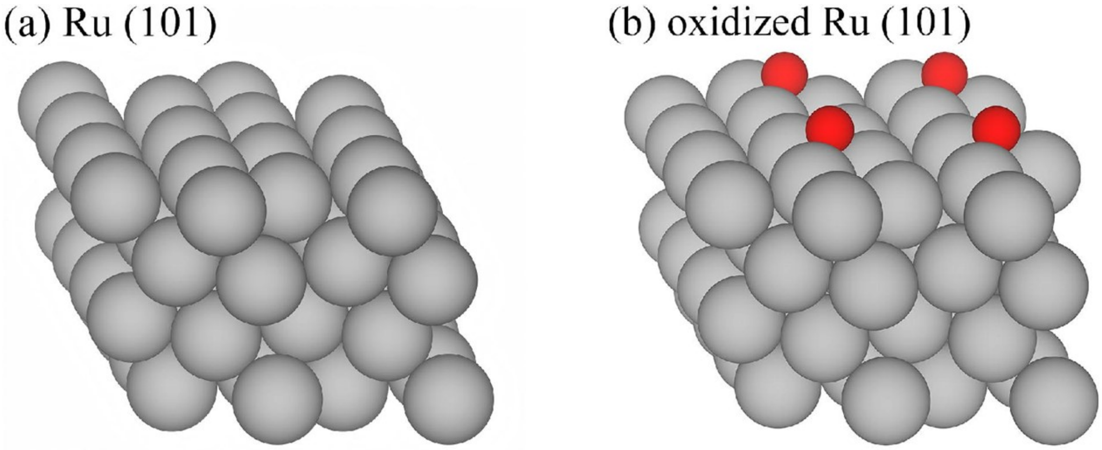

Fig. S13. The Optimized configurations of (a) pristine Ru (101) surface and (b) partially oxidized Ru (101).

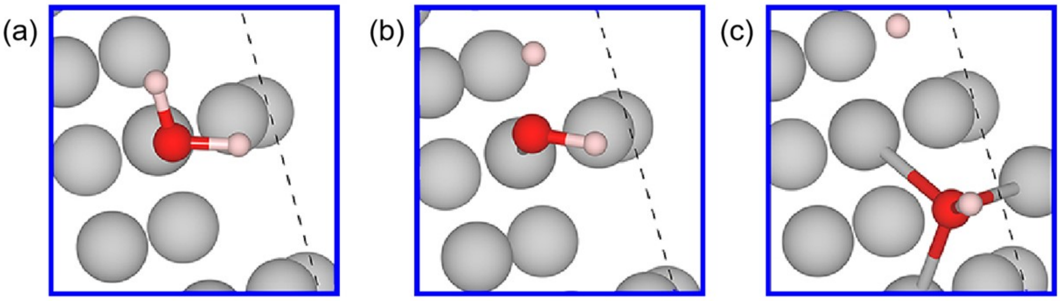

Fig. S14. The structures of (a) initial states, (b) transition states and (c) final states on Ru for water dissociation barriers

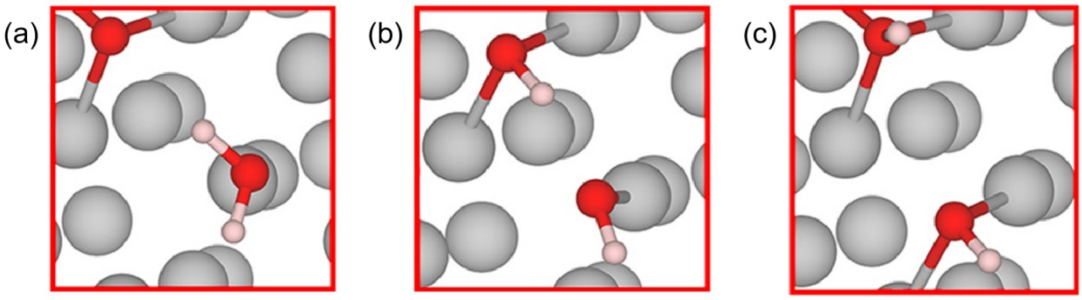

Fig. S15. The structures of (a) initial states, (b) transition states and (c) final states on oxidized Ru for water dissociation barriers

Table S1. The results of deconvolution of the Ru $3d_{5/2}$ and O $1s$ XPS spectra of different catalysts.

	Ru $3d_{5/2}$			O $1s$		
	BE/eV	Area proportion (to Ru^0)	FWHM	BE/eV	Area proportion (to O_L)	FWHM
Ru/C	280.6 (Ru^0)	1	0.81	530.2 (O_{Lat})	1	0.84
	281.0 (Ru^{4+})	0.50	1.24	531.3 (O_V)	2.25	2.15
				532.7 (O_{Abs})	3.13	1.87
Ru/C-220	280.4 (Ru^0)	1	0.80	530.0 (O_{Lat})	1	1.15
	281.2 (Ru^{4+})	1.64	1.01	531.5 (O_V)	0.89	2.22
				533.00 (O_{Abs})	0.75	2.54

Table S2. Comparison of the overpotential and corresponding Tafel slope with recently reported Ru-based catalysts in alkaline conditions.

	Electrocatalyst	**Overpotential**	**Tafel slope (mV**	**Refs.**
1	**Ru/C-220**	**18**	**34.9**	**This work**
2	**Ru/C**	**54**	**56.2**	
3	RuAu SAA	24	37	Adv. Energy Mater.
4	$RuRh_2$ bimetallene	24	31	Adv. Sci. 2021, 8,
5	Ru-O-MoS_2	50	45	Chem. Sci., 2024, 15,
6	Ru-MoO_2	29	31	J. Mater. Chem. A.
7	Mo_2C-Ru/C	22	25	Adv. Funct. Mater.
8	Pd-Ru@NG	28	73	Chem. Commun. 2019,
9	Ru/NC-400	39	49	Adv. Funct. Mater.
10	Ru-Mo_2C-CN	34	80	J. Catal. 2020, 392, 313.
11	Ru-MoS_2-Mo_2C-TiN	25	58	Nano Energy. 2021, 88,
12	Ru@CN-0.16	32	53	Energy Environ. Sci.
13	Ru-NGC	37	40	Chem. Commun. 2019,
14	HP-Ru/C	25	29	Appl. Catal., B. 2021,
15	O_2-Ru-N_2	10	45.6	Chem. Mater. 2024, 36,
16	NiO/Ru@Ni	39	75	J. Mater. Chem. A.

Table S3. Comparison of the impedance of different catalysts.

Sample	R_s (ohm)	R_{ct} (ohm)
Pt/C	5.3	16.3
Ru/C	5.4	30.9
Ru/C-200	5.1	5.8
Ru/C-220	5.1	4.4
Ru/C-240	5.2	14.6

References

1. Z. Lu, W. Xu, W. Zhu, Q. Yang, X. Lei, J. Liu, Y. Li, X. Sun and X. Duan, *Chem. Commun.*, 2014, **50**, 6479-6482.
2. Q. Xiang, F. Li, W. Chen, Y. Ma, Y. Wu, X. Gu, Y. Qin, P. Tao, C. Song, W. Shang, H. Zhu, T. Deng and J. Wu, *ACS Energy Lett.*, 2018, **3**, 2357-2365.
3. G. Kresse and J. Furthmuller, *Phys. Rev. B*, 1996, **54**, 11169-11186.
4. G. Kresse and J. Furthmuller, *Comput. Mater. Sci.*, 1996, **6**, 15-50.
5. P. E. Blochl, *Phys. Rev. B*, 1994, **50**, 17953-17979.
6. J. P. Perdew, K. Burke and M. Ernzerhof, *Phys. Rev. Lett.*, 1996, **77**, 3865-3868.
7. G. Henkelman, B. P. Uberuaga and H. Jónsson, *J. Chem. Phys.*, 2000, **113**, 9901-9904.
8. P. E. Blochl, O. Jepsen and O. K. Andersen, *Phys. Rev. B*, 1994, **49**, 16223-16233.
9. V. Wang, N. Xu, J. C. Liu, G. Tang and W. T. Geng, *Comput Phys Commun*, 2021, **267**, 108033.